Inter-Symbol Interference Analysis in Neuro-Synaptic Communications

Abolfazl Amiri† and Behrouz Maham‡
†School of ECE, College of Engineering, University of Tehran, Iran
‡Department of Electrical and Electronic Engineering, School of Engineering, Nazarbayev University, Astana, Kazakhstan
Email: aamiri@ut.ac.ir, behrouz.maham@nu.edu.kz

***Abstract*—Neuro-synaptic communication system has a vital role in transporting information in the body nervous system. This system uses electrical pulses and neurotransmitters as its information carriers and sends them through the body neural network. Some illnesses like seizures, epilepsy and multiple sclerosis corrupt data transmission by adding extra interference, making it unstable. In this paper, we propose an inter-symbol interference (ISI) model for neuro-synaptic communication system and then, by designing various equalizers, try to compensate the effect of the ISI in the receiving neuron. The effect of the equalization is compared with the system without the equalizer, and the performance improvement is remarkable. We also calculate the appropriate sampling time for this system to make external digital systems capable of interconnecting with neuro-synaptic system.**

Keywords: Molecular communication, Neuro-spike, Inter symbol interference, Equalizer, Seizures and epilepsy

I. Introduction

The concept of molecular communication, that has been proposed in recent years, is a new paradigm in communication which describes communications between very small scale organs and machines [1]. In this communication system, molecules carry information between nano-machines like calcium signaling, pheromones and neurotransmitters [2]. Among these systems, a vast biological communication system is neuro-synaptic communications which controls the data transmission between the brain and other body organs in the nervous systems. This system uses electrical impulses and neurotransmitters to carry information between the neurons and synaptic areas.

Fig. 1 shows a neuron cell in the body neural network. The three main parts of a neuron are soma, dendrites and axon. Spikes are generated in soma, and then, they are propagated in axon to reach their destinations. A burst is a series of action potentials, a short-lasting event in which the electrical membrane potential of a cell rapidly rises and falls [3], fired in rapid succession [4]. Burst activities have important roles in our body, like generation of sleep rhythms [5], enhancing reliability of synaptic transmission, noise filtering and etc. Another example is in visual information encoding, in which bursts may signal the detection of objects to the cortex while tonic firing may serve in the encoding of object details.

In the communication theory, transferring data in the band limited channels, i.e. channels which have finite bandwidth, may cause Inter Symbol Interference (ISI) [19]. This interference occurs when the bandwidth of the data is larger than the channel, so the adjacent transmitted symbols distort each other. In the nervous system, we have a band limited channel which causes ISI in high transmission rates, like bursts, to the original data.

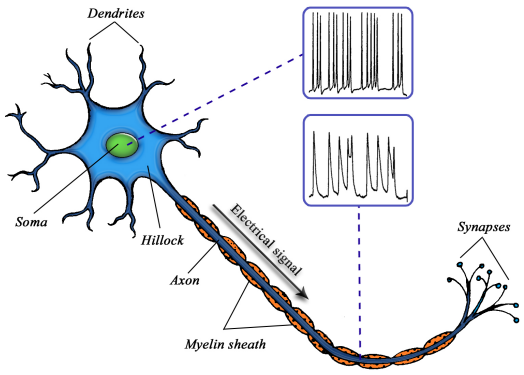

Fig. 1. Schematic of a neuron cell. The ISI can cause distortion to adjacent spikes.

Some diseases like multiple sclerosis (MS), seizures and epilepsy [6] and [7] cause defects in the nervous system and damage neurons. These illnesses cause disorders to the neuro-synaptic communication system, making it dysfunctional to transmit or detect correctly in the neural system. These factors can cause extra interference in the signals and deteriorate the correct patterns in the spike transmission. For example, MS damages the myelin covering the axon and makes it vulnerable to interference from the other neurons. One of the causes for seizures and epilepsy is the interference between the spikes, which makes their amplitude large enough to unstabilize the nervous system and create dangerous conditions for the patient. In [8], the analysis for synaptic interference channels and their achievable communication rates have been provided. The authors in [9] proposed a simple expression for the ISI in this communication system. Here, we focus on the somatic and the axonal transmissions, in which Inter Symbol Interference could occurred during the burst activities. The discussed illnesses such as epilepsy cause external interference to body nervous system and we manage to design equalizers to prevent the effect of this disorder.

The main goal of this work is to design an optimum receiver and equalizer to cancel the effect of the inter symbol interference caused by the transmission through the band limited

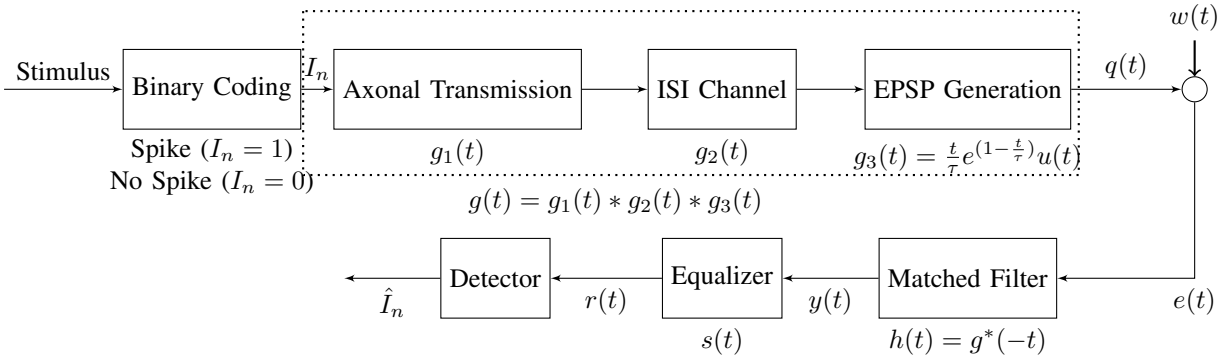

Fig. 2. The physical channel model of a neuro-synaptic communications channel.

channel and detecting the original signal. We also compare the performance of different kinds of equalizers in different channel models and various types of neural receptors. First, we propose a novel system model, which models the ISI channel and the effect of the axonal transmission. Then, we show the improvement of decision system due to the equalization and compare it with the case of using no equalizer and symbol by symbol detection and also with an ideal system with no ISI and flat frequency response. We can use the proposed method as a therapeutic approach for the patents suffer from mentioned disorders. Moreover, we find an appropriate sampling time for neuro-synaptic system by Nyquist criterion in order to interconnect digital devices to this communication system.

II. System Model

In Fig. 2, a neuro-synaptic communication system model for a neuron in pyramidal cell is illustrated. At the input of this model, receptors of dendrites receive neurotransmitters, chemical messengers in the synaptic area, from presynaptic neurons. The spike train has a binary feature, in which occurring an spike has the bit value of $I_n = 1$ and with no spike we have $I_n = 0$. Thus, the binary coding block uses this property to encode the information and it is also like the on-off keying modulation with delta-Dirac like pulses. There are two kinds of receptors: ionotropic receptors and metabotropic receptors. Ionotropic neurotransmitter receptors can be excited or be inhibited due to the types of diffused neurotransmitters reaching them. On the other hand, metabotropic receptors only modulate the actions of excitatory and inhibitory neurotransmitters and they are neither excitatory nor inhibitory. Excitation of these receptors generates electrical potentials. These potentials are summed up in a temporal or spatial manner in soma and if their aggregated potential reaches the desired threshold, an action potential (AP) would be generated by the soma in the neuron [10].

After the axon hillock (see Fig.1), the pulse train enters the axon on their way through the neuron cell. The axon could be modeled as a second order low pass butterworth filter [3]. This low-pass filtering property also justifies the refractory period of the axon, in which prevents spikes from traveling back in the axon. This filter's normalized transfer function is given as

$$G_1(j\omega) = \frac{d_0}{d_0 - \omega^2 + 2d_1 j\omega}[u(j\omega) - u(j\omega - d_2)] \qquad (1)$$

where $d_0, d_1$and d_2 coefficients could be determined by experimental data sets presented in [11].

In order to convert this filter to a digital one, first, we modify the coefficients so that the absolute value of $G_1(j\omega)$ in $\omega = d_2$ approaches zero. Thus, we can eliminate the step functions in (1). Then by using the bilinear method proposed in [12], the corresponding digital filter is as follows

$$\begin{aligned} G_1(z) &= G_1(j\omega)\big|_{j\omega=\frac{2}{T_{\text{sample}}}\frac{1-z^{-1}}{1+z^{-1}}} \\ &= \frac{d_0'}{d_0' + s^2 + d_1' s}\big|_{s=j\omega} \\ &= T_{\text{sample}}^2 \frac{1 + 2z^{-1} + z^{-2}}{m_1 + m_2 z^{-1} + m_3 z^{-2}}, \end{aligned} \qquad (2)$$

where d_0' and d_1' are new coefficients of the continuous time filter, in which we modify to eliminate the step function and $m_1 = d_0' T^2 + 2T d_1' + 4$, $m_2 = 2d_0' T^2 - 8$ and $m_3 = d_0' T^2 - 2d_1' T + 4$ are denominator coefficients of the digital filter.

Spike trains can form all kinds of patterns, such as rhythmic spiking and bursting and often display oscillatory activity [13]. In addition to the action potentials which are rapidly changing waves, there are other kinds of more slowly changing waves that follow in the succession like after hyper polarisation (AHP) and depolarizing after potentials (DAP). An AHP acts as an inhibitory feedback for soma which by increasing the potential difference between soma and the other parts of the neuron, it decreases the probability of another action potential. A fast AHP leads to a large current being sourced back into the soma and initiating a DAP [4].

A refractory period is a period of time which an organ or cell is incapable of repeating a particular action. In a more precisely description it is the amount of time that takes for an excitable membrane to be ready for a second stimulus once it returns to its resting state following an excitation. It most commonly refers to electrically excitable muscle cells or the neurons [14]. In some backpropagation activities in neurons, successive DAPs aggregate together and cause to increase the frequency of somatic spike generation. This results in reaching the threshold and generating of a high frequency somatic spike

doublet or triplet. Since the refractory period in the dentritic and the axonal parts of the neuron is longer than the somatic one, they can not support the propagation of doublet [4]. We model this feature with an ISI channel which has the transfer function $g_2(t)$. In the rest of the paper, we use the discrete time model for our system and also we use capital symbols for each block showing their corresponding Z-transforms. A general form of an ISI channel in Z-transformed domain is represented as:

$$G_2(z) = \sum_{i=0}^{L} \alpha_i z^{-i}, \tag{3}$$

where α_i's are channel gains for the delayed versions of the original pulse and L is the length of channel's memory. As shown in Fig. 3, this memory sums up adjacent symbols with each other and causes distortion on the transmitting signal.

As illustrated in Fig.4 in [15], we can see at most two or three symbols interfere with each other. This observation will help us estimating the memory length of the channel. As mentioned in [3], in the high frequency firing rates with lower inter symbol intervals, the amplitude of the consecutive spikes decreases logarithmically. Using this fact, we can model α_i's in (3) with exponentially decaying characteristic of the form

$$\alpha_i = \sqrt{1-a^2}\, a^i, \quad i = 0, 1, ..., L\ , \tag{4}$$

where a is a real constant we can determine using data in [15] and [16].

The normalized analog voltage waveform generated at the receptors of the post-synaptic terminal, i.e. receiver side, in response to the neurotransmitters, or in other words our pulse shaping function is in the form of [17]

$$g_3(t) = \frac{t}{\tau} \exp{(1 - \frac{t}{\tau})} u(t), \tag{5}$$

where $u(t)$ is step function and τ is some constant and its value in $g_3(t)$, which is called $alphafunction$ in the EPSP generation, is associated with the type of the receptor. For example, if we name time constants of ionotropic receptors like Alpha-Amino-3-Hydroxy-5-Methyl- 4-Isoxazole-propionate (AMPA) and N-Methyl-D-Aspartate (NMDA) with τ_A and τ_N, respectively, then we would have $\tau_N > \tau_A$ [3].

Note that, the sampling rate for discretizing the model should be chosen proportional to the bandwidth of the EPSP pulse shape. According to the Fourier transform of $g_3(t)$ which is $G_3(f) = \frac{\exp 1}{\tau(\frac{1}{\tau}+j2\pi f)^2}$, the sampling rate is related to the value of τ. The 3-dB frequency of this transfer function is $f_{3dB} = \frac{\sqrt{\sqrt{2}-1}}{2\pi\tau}$, and thus, the sampling period is

$$T_{\text{sample}} = \frac{1}{2 f_{3dB}} = \frac{\pi\tau}{\sqrt{\sqrt{2}-1}} \approx 4.88\,\tau. \tag{6}$$

This sampling time could be used in practical systems to employ digital circuits interconnecting the neurons.

Through the transmission of the pulses along soma, axon and synapses, and because of the ionic exchanges, noise adds to the original signal. We model this with an additive Gaussian white noise $w(t)$ [18].

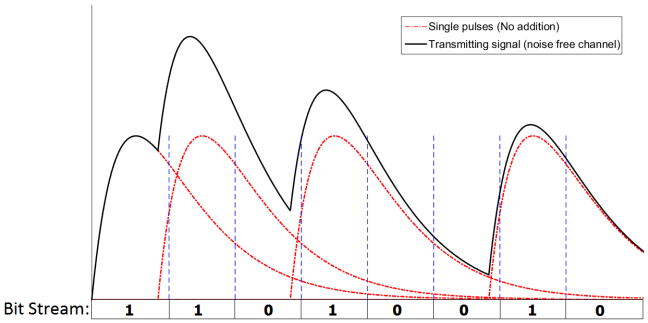

Fig. 3. Effect of channel memory on distortion of transmitting signal.

For maximizing the signal to noise ratio (SNR), we used a filter matched to the equivalent channel impulse response which the input information sequence, I_k, sees at the input of the model. This impulse response is equal to $g(t) = g_1(t) * g_2(t) * g_3(t)$. Thus, the desired matched filter's impulse response is $h(t) = g^*(-t)$ and the output of this block is sampled at $t = kT_{\text{sample}}$, for $k = 1, 2, \cdots$.

The equivalent channel for the input binary string is

$$c(t) = g(t) * h(t) = g(t) * g^*(-t). \tag{7}$$

Hence, the output of the matched filter becomes

$$y_n = \sum_{k=-\infty}^{\infty} I_k c_{n-k} + z_n\ , \tag{8}$$

where the subscript notation shows the sampled version of the variable in $t = nT$ timescale and $z_n = w_n * c_n$ is a colored Gaussian noise. The next block in Fig.2 is an equalizer that reduces the effect of other symbols on current transmitted symbol.

III. Symbol by Symbol Detection

Before discussing the equalization, we first derive the performance of a plain system with no equalizer. The purpose of this section is to find a bound for bit error rate to compare with the results of next parts which we use the equalizer to compensate the effect of ISI.

If we sample the signals with an appropriate rate, which we derive in (6), we can treat $G_1(j\omega)$ as a flat filter. Thus, for finding the values of $c(t)$ in (7), we just incorporate the G_2 and G_3 systems. By applying the inspection method [12], discrete time values could be found. We rewrite (8) with the dominant interfering symbols, which is based on the practical data provided in [16], it can be expressed in following form:

$$y_n = c_0 I_n + c_1 I_{n-1} + z_n. \tag{9}$$

Thus, we just need two values of c_n to calculate the output of channel. Assuming the ISI channel with $\alpha_0 = 1$, $\alpha_1 \neq 0$ and $\alpha_i = 0$ for $i > 1$, the overall system coefficients (c_n's) would be

$$\begin{aligned} c_0 &= T^4 \frac{5\alpha_1 + 1 - m_2 m_4 (m_1 + m_3)}{m_1 m_3} \\ c_1 &= T^4 \frac{7\alpha_1 + 4 - m_4 m_5 - c_0 m_2 (m_1 + m_3)}{m_2 (m_1 + m_3)}\ , \end{aligned} \tag{10}$$

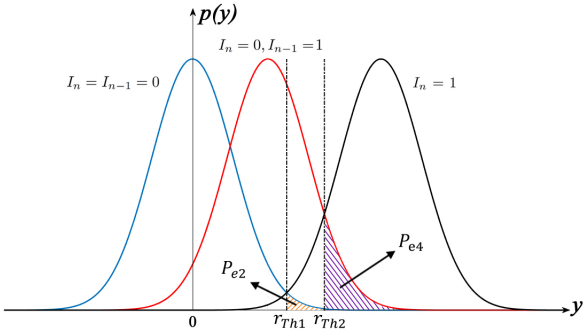

Fig. 4. The probability distribution for y in the ISI axonal channel. Here, the error probability for two cases , in which described as P_{e2} and P_{e4} in the text, has been illustrated. The value for r_{TH_1} is $\frac{c_0\sqrt{\mathcal{E}}}{2}$ and also $r_{TH_2} = \frac{(c_0+c_1)\sqrt{\mathcal{E}}}{2}$.

where $m_4 = \frac{4\alpha}{m_1 m_3}$ and $m_5 = m_1^2 + m_2^2 + m_3^2$. The variance of the noise z_n in (9), is $\sigma_z^2 = c_0 \frac{N_0}{2}$, where we assume the noise power spectral density to be $N_0/2$. Here, by implementing the symbol by symbol detection method, for calculating the probability of error, we have four cases according to the values of I_n and I_{n-1}. If we transmit $I_n = 1$ with $\sqrt{\mathcal{E}_b}$ and $I_n = 0$ with 0, the decision threshold for the case without ISI, from Maximum Likelihood (ML) criterion would be $c_0\sqrt{\mathcal{E}_b}/2$. But here, according to the channel response we should modify threshold values. For the first case, we assume $I_n = I_{n-1} = \sqrt{\mathcal{E}_b}$, thus:

$$\begin{aligned} P_{e_1} &= P(e|I_n = I_{n-1} = \sqrt{\mathcal{E}_b}) \\ &= P(y_n < \frac{\sqrt{c_0\mathcal{E}_b}}{2}|I_n = I_{n-1} = \sqrt{\mathcal{E}_b}) \\ &= P\Big(z_n < \sqrt{\mathcal{E}_b}\big(-c_0 - 2c_1\big)\Big) \\ &= Q\left(\sqrt{\frac{\mathcal{E}_b}{2c_0N_0}(c_0 + 2c_1)^2}\right), \end{aligned} \tag{11}$$

where $Q(x) = \frac{1}{\sqrt{2\pi}}\int_x^\infty \exp\frac{-u^2}{2}du$ is Q-function. Similarly other error probabilities can be calculated:

$$\begin{aligned} P_{e_2} &= P(e|I_n = I_{n-1} = 0) \\ &= Q(\sqrt{\frac{c_0\mathcal{E}_b}{2N_0}}) \\ P_{e_3} &= P(e|I_n = \sqrt{\mathcal{E}_b}, I_{n-1} = 0) \\ &= Q(\sqrt{\frac{c_0\mathcal{E}_b}{2N_0}}) \\ P_{e_4} &= P(e|I_n = 0, I_{n-1} = \sqrt{\mathcal{E}_b}) \\ &= Q\left(\sqrt{\frac{\mathcal{E}_b}{2c_0N_0}(c_0 - 2c_1)^2}\right), \end{aligned} \tag{12}$$

and finally the overall probability of error would be:

$$P_{e_{\text{no equalizer}}} = \frac{1}{4}(P_{e_1} + P_{e_2} + P_{e_3} + P_{e_4}). \tag{13}$$

Fig. 4 shows the optimum receiver threshold for $I_n = I_{n-1} = 0$ and $I_n = 0, I_{n-1} = 1$ cases. In addition, the error probability of an ideal channel with no ISI and flat frequency response $(c_0 = 1, c_1 = 0)$ would be the simple error probability formula for binary Pulse Amplitude Modulation (PAM) which is

$$P_{e_{\text{ideal channel}}} = Q(\sqrt{\frac{d_{min}^2}{2N_0}}) = Q(\sqrt{\frac{\mathcal{E}_b}{2N_0}}), \tag{14}$$

where d_{min} is equal to the minimum distance of points in PAM constellation, which equals to $\sqrt{\mathcal{E}_b}$.

IV. Equalizer Design for Interference Cancellation

In this section, we study the performance of our neural system, using three different designs of equalizers. We first consider the linear equalizers and for tap weight coefficient optimization, we will use two criteria: one is the peak distortion and the other is the mean-square-error criterion.

A. Peak Distortion Criterion

This method tries to minimize the peak distortion which occurs at worst case ISI in output of the equalizer.This output occurs during consecutive APs and it could cause instability in system and initiate an epilepsy attack. To deal with nonwhite noise, we use a whitening filter before equalizer and to find it's frequency response, we first decompose the channel response in this form

$$C(z) = R(z)R^*(\frac{1}{z^*}), \tag{15}$$

in which we use stable poles and zeros to construct $R^*(\frac{1}{z^*})$. The equivalent response for whitening filter cascaded with zero forcing equalizer that cancels all other symbols is given by

$$S_1(z) = \frac{1}{R(z)R^*(\frac{1}{z^*})} = \frac{1}{C(z)}. \tag{16}$$

For zero forcing equalizer with infinite number of taps, the value of SNR is given by [19]:

$$SNR_\infty = \left[\frac{TN_0}{2\pi}\int_{-\pi/T}^{\pi/T}\frac{d\omega}{C(e^{j\omega T})}\right]^{-1}. \tag{17}$$

This kind of equalizer has noise enhancing property at high SNR regimes. For finite length zero forcing equalizer, we try to make the output of the equalizer to just keep the main information bit and remove interfering terms. the discrete time model of the output of an equalizer with $2K+1$ taps is:

$$r_n = \sum_{i=-K}^{K} s_n y_i. \tag{18}$$

Thus, we can solve the above equation by using its matrix form, which is

$$\boldsymbol{sP = r \ \rightarrow s = P^{-1}r}, \tag{19}$$

where r is $2K+1$ zero vector with just a one in its $(K+1)$th element, s is coefficient vector of equalizer and $\boldsymbol{P}$ is a $(2K+1)\times(2K+1)$ matrix with following elements:

$$P = [y(d), y(d+1), ..., y(d+2K)], \tag{20}$$

where $y(d)$ means to circularly shift the output of the matched filter $y(t)$ in order to make its biggest element to be its first one, also other rows of this matrix made by shifting the above row one unit to right.

B. Mean-Square-Error (MSE) Criterion

The objective of MSE is to minimize the mean square value of the error $\epsilon_n = I_n - \hat{I}_n$. By solving this optimization problem and using the orthogonality of error to signal sequence will lead us to equivalent whitening filter and MSE equalizer with following response

$$S_2(z) = \frac{1}{C(z) + N_0}\,, \tag{21}$$

note that (21) specifies an equalizer with infinite number of taps. In finite tap case and with $2M+1$ tap coefficients, we must solve a matrix equation in the form

$$\mathbf{\Gamma S_2} = \boldsymbol{\xi}\,, \tag{22}$$

where $\mathbf{\Gamma}$ is $(2M+1)\times(2M+1)$ covariance matrix and ξ is a $(2M+1)$ vector with elements given in [19]. This equation leads to inversion of $\mathbf{\Gamma}$ matrix and then we obtain the optimum tap coefficients. To find SNR value at the output of these equalizers, first we evaluate the value of MSE ($E\{|\epsilon_n|^2\}$) and then we reach to SNR value. After a few mathematical work we have

$$SNR_\infty = \frac{\sum_{k=-\infty}^{\infty} s_{2_k} r_{-k}}{1 - \sum_{k=-\infty}^{\infty} s_{2_k} r_{-k}}\,, \tag{23}$$

and

$$SNR_{(2K+1)tap} = \frac{\xi^H \Gamma^{-1} \xi}{1 - \xi^H \Gamma^{-1} \xi}\,, \tag{24}$$

where in (23) r_k is discrete time domain equivalent of $R(z)$ and H in (24) represents the conjugate transpose.

C. Decision Feedback Equalizer (DFE)

In this subsection, we propose a nonlinear equalizer for our model which uses one filter in feed forward path and one in feedback path, so we have two degrees of freedom for tap coefficient optimization in our design. For infinite tap mode, [20] showed that the optimum equalizer is similar to ZF mode, so we focus on the finite tap mode with M_1+1 taps in forward direction and M_2 taps in backward path. Again by using MSE criterion and with a scenario similar to the previous section, first we optimize feed forward filter coefficients and according to them we decide on the feedback ones. As described in [19], the solution to this problem with $M_1 + M_2 + 1$ optimization variable is given by solving following linear equations:

$$\sum_{i=-M_1}^{0} \psi_{ki} s_i = r^*_{-k}, \quad \text{for } k = -M_1, ..., -1, 0, \tag{25}$$

where

$$\psi_{ki} = \sum_{j=0}^{-k} r^*_j r_{j+k-i} + N_0\,\delta_{ki}, \quad \text{for } k, i = -M_1, ..., -1, 0, \tag{26}$$

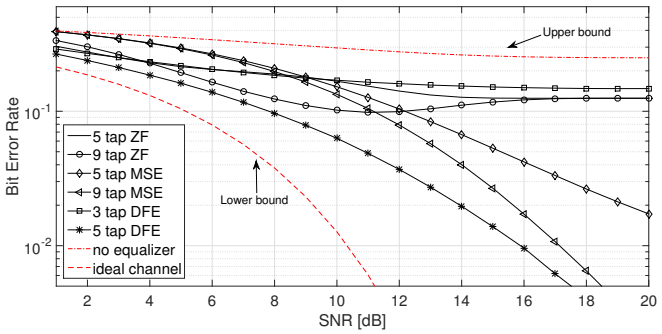

Fig. 5. Performance analysis of zero-forcing, mean square error and decision feedback equalizers with ideal channel and no equalization mode (Burst probability = 0.5, $\alpha_0 = 1$, $\alpha_1 = 0.8$ and $\tau_A = 1$).

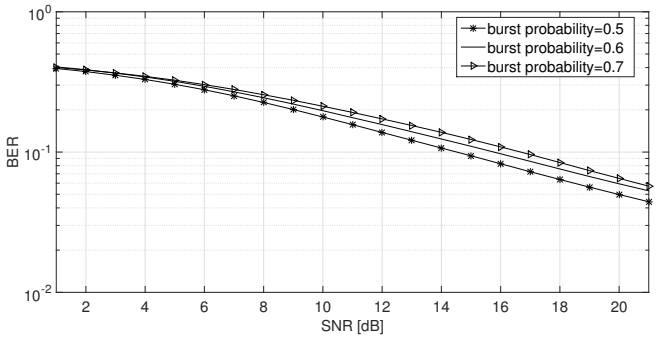

Fig. 6. Performance analysis of MSE equalizer with different burst probabilities (Number of taps =7, $\alpha_0 = 1$, $\alpha_1 = 0.8$ and $\tau_A = 1$).

to find feed forward filter taps. In (26), δ_{ki} is Dirac delta function. Now, we use this coefficients to obtain feedback equations in the form of

$$s_l = -\sum_{i=-M_1}^{0} s_i r_{l-i}, \quad \text{for } l = 1, 2, ..., M_2. \tag{27}$$

V. Simulation Results

In this section, we evaluate the analytical expressions obtained in previous sections. First, we compare the bit error rate results of equalizers with different number of taps in non-ideal channel with the case we do not use the equalization and with an ideal channel without ISI. Fig. 5 illustrates this property, in which we have used first order delay channel with $\alpha_1 = 0.8$ according to burst spikes interference data in [16]. We also use the equiprobable signal in source firing neuron and $c_0 = 0.95$ and $c_1 = 0.6$ for simulation setup. As we expect, in all designs, as the number of taps increases, we see improvements in equalizer performance.

To compare the performance of system, employing these equalizer, we observed that the MSE equalizer, acts better than ZF in higher SNRs and also DFE equalizer, performs better versus MSE with equal number of taps, and this is because of the error feedback and correction feature of these kinds of equalizers that reduces the number of burst errors. Note that we also employ a 3-tap DFE equalizer which performs worse than a 5-tap ZF one, it is because of the fact that the equalizer

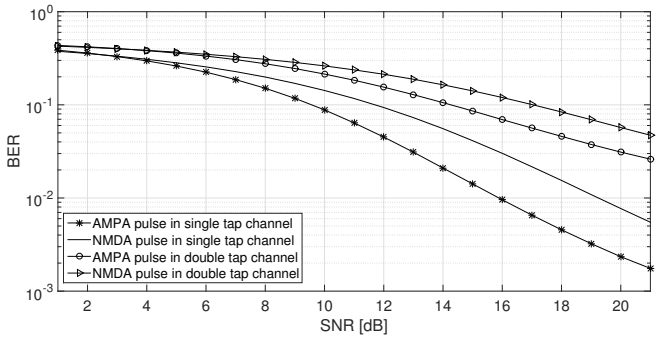

Fig. 7. Performance analysis of MSE equalizer with different pulse shapes and channel models (Burst probability=0.5, Number of taps =7, $\alpha_0 = 1$, $\alpha_1 = 0.8$, $\alpha_2 = 0.6$, $\tau_A = 1$ and $\tau_N = 3$).

could not compensate the channel's memory with its taps and a residual ISI is present even in high SNRs. As you can see with no equalization, we reach an upper bound or a worst case in bit error rate and also in ideal channel we reach a lower bound on it in which we try to reach it by equalizers.

Then we change the spike generation probability in central nervous system to create more dense bursts and evaluate our equalizer's response in interference cancellation. Again we use $\alpha_1 = 0.8$ for channel model. Note that in this case because of the different probabilities in signal generation, we should use maximum a posteriori probability rule, or MAP rule with decision threshold:

$$r_{th} = \frac{1}{c_0\sqrt{\mathcal{E}_b}}\left(\frac{N_0}{2}\ln(\frac{1-p}{p}) + \frac{c_0^2}{2}\mathcal{E}_b\right), \qquad (28)$$

where $\mathcal{E}_b$ represents the energy of the transmitted signal and p is the probability of spike generation. It is obvious that in equiprobable signaling we have $r_{th} = \frac{c_0\sqrt{\mathcal{E}_b}}{2}$. In Fig. 6 we compare the performance of 7-tap MSE equalizer with three different spike fire probabilities. As the probability increases we have more spikes interfere with each other and also reduction in system performance.

Finally, we compare the effect of different types of receptors and channel delays in ISI and equalizer output. As we mention in section II, time constant of NMDA receptors are greater than time constant in AMPAs, so we have a pulse with larger tale in NMDA mode which can cause more interference to other symbols. As you can see in Fig. 7, we compare these two pulse shapes in two different channels, one a single delay tap α_1 value used in previous simulations, and another channel with double tap delay property and $\alpha_2 = 0.6$. Equalizer performance diminishes as the channel delay or memory increases and also with NMDA pulse, we face more error rate due to wide pulses overlapping each other.

VI. Conclusion

In this paper, we investigated the effect of inter symbol interference in neuro-synaptic communication system. We have seen that some illnesses cause external interference to the system and we managed to design equalizers to prevent the effect of this disorder. We also compared the performance of the different types of the equalizers for multiple kinds of channels and the neural characteristics and observed its performance improvements against the case with no equalization. The analysis could be extended to multiple access interference management in neural network of the body. Future advances in the nano-technology will help us implement these compensation systems in neural network to help cure nervous disorders.

References

[1] I. F. Akyildiz, F. Brunetti, and C. Blázquez, "Nanonetworks: A new communication paradigm," *Computer Networks*, vol. 52, no. 12, pp. 2260–2279, Aug. 2008.

[2] A. Enomoto, M. Moore, T. Nakano, R. Egashira, T. Suda, A. Kayasuga, H. Kojima, H. Sakakibara, and K. Oiwa, "A molecular communication system using a network of cytoskeletal filaments," in *Proceedings of the NSTI Nanotechnology Conference*, vol. 1, May 2006.

[3] E. Balevi and O. B. Akan, "A physical channel model for nanoscale neuro-spike communications," *IEEE Transactions on Communications*, vol. 61, no. 3, pp. 1178–1187, Mar. 2013.

[4] J. Feng, *Computational neuroscience: a comprehensive approach*. CRC press, 2003.

[5] G. B. Ermentrout and D. H. Terman, *Mathematical foundations of neuroscience*. Springer Science & Business Media, 2010, vol. 35.

[6] A. Compston and A. Coles, "Multiple sclerosis," *The Lancet*, vol. 372, no. 9648, pp. 1502–1517, Oct. 2008.

[7] R. S. Fisher, W. V. E. Boas, W. Blume, C. Elger, P. Genton, P. Lee, and J. Engel, "Epileptic seizures and epilepsy: Definitions proposed by the international league against epilepsy (ILAE) and the international bureau for epilepsy (IBE)," *Epilepsia*, vol. 46, no. 4, pp. 470–472, Apr. 2005.

[8] D. Malak and O. B. Akan, "Synaptic interference channel," *IEEE International Conference on Communications Workshops (ICC)*, pp. 771–775, June 2013.

[9] Q. Liu, P. He, K. Yang, and S. Leng, "Inter-symbol interference analysis of synaptic channel in molecular communications," pp. 4424–4429, June 2014.

[10] D. Purves, E. M. Brannon, R. Cabeza, S. A. Huettel, K. S. LaBar, M. L. Platt, and M. G. Woldorff, *Principles of cognitive neuroscience*. Sinauer Associates Sunderland, MA, 2008.

[11] M. Raastad and G. M. Shepherd, "Single-axon action potentials in the rat hippocampal cortex," *The Journal of physiology*, vol. 548, no. 3, pp. 745–752, May 2003.

[12] A. V. Oppenheim, R. W. Schafer, and J. R. Buck, *Discrete-time Signal Processing (2Nd Ed.)*. Upper Saddle River, NJ, USA: Prentice-Hall, Inc., 1999.

[13] X.-J. Wang, "Neurophysiological and computational principles of cortical rhythms in cognition," *Physiological reviews*, vol. 90, no. 3, pp. 1195–1268, July 2010.

[14] H. W. Heiss, "Human physiology," *Clinical Cardiology*, vol. 6, no. 9, pp. A43–A44, Sep. 1983.

[15] N. Lemon and R. W. Turner, "Conditional spike backpropagation generates burst discharge in a sensory neuron," *Journal of Neurophysiology*, vol. 84, no. 3, pp. 1519–1530, Sep. 2000.

[16] E. M. Izhikevich, *Dynamical systems in neuroscience*. MIT press, 2007.

[17] P. Dayan and L. F. Abbott, *Theoretical neuroscience*. Cambridge, MA: MIT Press, 2001, vol. 806.

[18] B. Maham, "A communication theoretic analysis of synaptic channels under axonal noise," *Communications Letters, IEEE*, vol. PP, no. 99, pp. 1–1, Sep. 2015.

[19] M. Salehi and J. Proakis, *Digital Communications*, ser. McGraw-Hill higher education. McGraw-Hill Education, 2007.

[20] C. Belfiore, J. H. Park Jr *et al.*, "Decision feedback equalization," *Proceedings of the IEEE*, vol. 67, no. 8, pp. 1143–1156, 1979.